Results from NA48/2 on $\pi\pi$ scattering lengths measurements in $K^{\pm} \to \pi^{+}\pi^{-}e^{\pm}\nu$ and $K^{\pm} \to \pi^{0}\pi^{0}\pi^{\pm}$ decays

Brigitte Bloch-Devaux[*][†]

IRFU/SPP, CEA-Saclay
E-mail: bbloch@hep.saclay.cea.fr

Very large statistics of charged kaon decays have been accumulated in 2003-2004 by the NA48/2 experiment at the CERN SPS. The analyses of $K^{\pm} \to \pi^{0}\pi^{0}\pi^{\pm}$ ($K_{3\pi}$) and $K^{\pm} \to \pi^{+}\pi^{-}e^{\pm}\nu$ (K_{e4}) decays give complementary approaches to the study of low energy $\pi\pi$ scattering. From data samples of 60 millions $K_{3\pi}$ and more than 1 million K_{e4} decays, precise values of a_{0} and a_{2}, the isospin 0 and 2 S-wave $\pi\pi$ scattering lengths, can be extracted with an unprecedented experimental precision of few percents, allowing accurate tests of Chiral Perturbation Theory predictions. The form factors of the K_{e4} decays and their energy dependence are also measured with an improved precision while the Dalitz plot parameters of the $K_{3\pi}$ decays are determined including a new quadratic term.

8th Conference Quark Confinement and the Hadron Spectrum
September 1-6, 2008
Mainz. Germany

[*]Speaker.

[†]On behalf of the NA48/2 collaboration: Cambridge, CERN, Chicago, Dubna, Edinburgh, Ferrara, Florence, Mainz, Northwestern, Perugia, Pisa, Saclay, Siegen, Turin, Vienna

1. Introduction

In the past years, $K^{\pm} \to \pi^+\pi^-e^{\pm}\nu$ decays (K_{e4}) were traditionally the cleanest laboratory to study $\pi\pi$ scattering close to threshold and extract the values of the S-wave scattering lengths. Two experiments collected sizable samples of K_{e4} decays: the Geneva-Saclay collaboration at the CERN/PS analyzed 30000 such K^+ decays [1] and the E865 collaboration at BNL about 400000 K^+ decays [2]. The NA48/2 collaboration at the CERN/SPS has collected more than one million decays in both charge modes in 2003-2004 and has already published results based on part of the data sample [3].

From $\sim$23 millions decays collected in the $K^{\pm} \to \pi^0\pi^0\pi^{\pm}$ mode ($K_{3\pi}$), the NA48/2 collaboration has already shown experimental evidence of a cusp-like structure in the $\pi^0\pi^0$ mass distribution at the $\pi^+\pi^-$ threshold [4]. This effect was interpreted as mainly due to charge exchange rescattering of the $\pi^+\pi^-$ system to $\pi^0\pi^0$, allowing an independent measurement of the $\pi\pi$ S-wave scattering lengths. Results based on the full data samples ($\sim$60 millions $K_{3\pi}$ and $\sim$1 million K_{e4} decays) will be presented here for both analyses. The form factors and $\pi\pi$ phase shift which characterize the K_{e4} decay are measured in a model independent method. S-wave $\pi\pi$ scattering lengths are then extracted with an improved precision using recent theoretical work [6] including isospin symmetry breaking effects. The slopes of the $K_{3\pi}$ Dalitz Plot are extracted together with the S-wave $\pi\pi$ scattering lengths and rely also on refined theoretical calculations [7, 8]. Both results are compared to previous K_{e4} measurements, to values obtained from a pionium life time experiment [9] and to the precise predictions from Chiral Perturbation Theory.

2. Experimental setup

Two simultaneous K^+ and K^- beams were produced by 400 GeV/c primary CERN/SPS protons, impinging on a beryllium target. The beams were then deflected in a front-end achromat to select momenta in the range (60 ± 3) GeV/c and focused at $\sim$ 200 m downstream in front of the first spectrometer chamber. A schematic view of the beam line and detector can be found in Ref. [10]. The NA48 detector and its performances are described elsewhere [5]. The main components used in the K_{e4} and $K_{3\pi}$ analyses are:

- a magnetic spectrometer consisting of a dipole magnet surrounded by two sets of drift chambers achieving a momentum resolution $\sigma(p)/p = (1.02 \oplus 0.044\,p)\%$ (p in GeV/c).

- a 27 radiation length liquid krypton calorimeter used to measure electromagnetic deposits and identify electrons through their E/p ratio. The transverse segmentation into 13248 projective cells gives an energy resolution $\sigma(E)/E = (3.2/\sqrt{E} \oplus 9.0/E \oplus 0.42)\%$ (E in GeV) and a space resolution for isolated showers $\sigma_x = \sigma_y = (0.42/\sqrt{E} \oplus 0.06)$ cm.

- a two plane segmented scintillator hodoscope allowing to trigger the detector readout on charged track topologies with a time resolution $\sim$150 ps.

- a neutral hodoscope consisting of a plane of scintillating fibers installed in the LKr calorimeter after 9.5 radiation lengths and divided into four quadrants.

- a two-level trigger logic selecting events with at least 3 tracks coming from a common vertex or one track and a minimum energy deposition in the calorimeter.

3. The K$_{e4}$ **decay analysis**

The data were selected for three well reconstructed charged track topologies, requiring two opposite sign pions and one e$^+$(e$^-$) identified from its E/p ratio. The reconstructed 3-track invariant mass (assigning a pion mass to each track) and p_t relative to the beam axis had to be outside an ellipse centered on the kaon mass and zero p_t, with semi-axes ± 20 MeV/c^2 and ± 35 MeV/c, allowing missing energy and p_t for the neutrino. No more than 3 GeV energy deposits in the calorimeter, non associated to tracks but in-time with the considered track combination, were allowed, keeping only a limited amount of soft radiative decays. The background sources are $K^\pm \to \pi^+\pi^-\pi^\pm$ decays with subsequent $\pi \to e\nu$ decay or a pion misidentified as an electron and $K^\pm \to \pi^\pm\pi^0(\pi^0)$ decays with subsequent Dalitz decay of a π^0 with an electron misidentified as a pion and photon(s) undetected. The fraction of Wrong Sign events (WS), $K^\pm \to \pi^+\pi^+e^\mp\nu$, which would violate the $\Delta S = \Delta Q$ rule, brings a direct control of the background level. The relative level of background/signal is $\sim 0.5\%$ and has been cross-checked using Monte Carlo simulation of the contributing background processes. This is illustrated in Figure 1 left with the distribution of the reconstructed beam momentum under the assumption of a missing neutrino .

3.1 Kinematics and analysis procedure

The K$_{e4}$ decay is fully described by the five kinematic Cabibbo-Maksymowicz variables [11]: two invariant masses $M_{\pi\pi}$ and $M_{e\nu}$ and three angles θ_π, θ_e and Φ as shown in Figure 1 right. Three axial (F, G, R) and one vector (H) complex form factors contribute to the transition amplitude expressed in terms of four other form factor combinations $(F1, F2, F3, F4)$ which can be then developed in a partial wave expansion of S, P-waves, identified with the phases of the $\pi\pi$ scattering [12]:

$$F = F_s\, e^{i\delta_s} + F_p\, e^{i\delta_p} \cos\theta_\pi, \quad G = G_p\, e^{i\delta_g}, \quad H = H_p\, e^{i\delta_h}.$$

The third axial form factor R is suppressed by a factor m_e^2/S_e. Consequently, there is no way to measure it in K$_{e4}$ decays but it is in principle accessible in K$_{\mu4}$ decays which are also recorded in this experiment. Assuming the same phase for F_p, G_p, H_p, only one phase and four real form factors are left ($\delta = \delta_s - \delta_p$, and F_s, F_p, G_p, H_p).

The event sample is then distributed over a grid of equal population boxes in the five-variable space . The chosen grid has ten bins in $M_{\pi\pi}$, five bins in $M_{e\nu}$, five bins in $\cos\theta_\pi$, five bins in $\cos\theta_e$ and twelve bins in ϕ, i.e. a total of 15000 five-dimensional boxes. Using the total sample of 739000 K$^+$ (411000 K$^-$) decays, there are 49 K$^+$ (27 K$^-$) per box. The Monte-Carlo simulation sample, 25 times larger than the data sample, takes into account acceptance, resolution effects as well as time-dependence of the beam geometry and experimental conditions. It also includes some of the electromagnetic effects, namely the classical Coulomb attraction between the two charged pions (expressed as the Gamow-Sommerfeld factor) and the emission of real photon(s) as described by the PHOTOS generator [13] interfaced to the simulation. In this analysis, the branching fraction is not measured, so only relative form factors are accessible: F_p/F_s, G_p/F_s, H_p/F_s and the phase shift δ. Without prior assumption on the shape of their variation with $M_{\pi\pi}$, the form factors and phase shift are measured in the independent $M_{\pi\pi}$ bins and do not depend upon any particular model. At
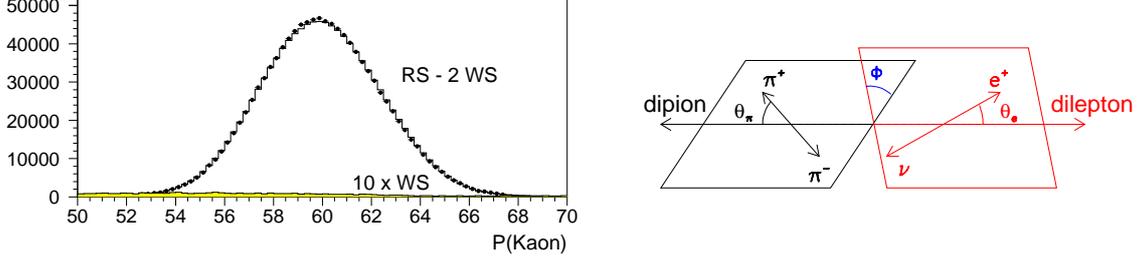
Figure 1: Left: Distribution of the reconstructed beam momentum (GeV/c). Data (background subtracted) are shown as symbols with error bars, simulation as open histogram and background (increased by a factor of 10 to be visible) from wrong sign events as shaded area. Right: Topology of the charged K_{e4} decay showing the angle definitions.

a second stage of the analysis, the observed variations of the form factors and phase shift with $M_{\pi\pi}$ are used to determine other parameter values through specific models.

Under the assumption of isospin symmetry, the form factors are developed in a Taylor expansion of dimensionless invariants q^2 ($q^2 = (S_\pi/4m_\pi^2) - 1$) and $S_e/4m_\pi^2$. The F_s form factor variation is described with three terms:

$$F_s = f_s \, (1 + f_s'/f_s \, q^2 + f_s''/f_s \, q^4 + f_e'/f_s \, S_e/4m_\pi^2)$$

while a q^2 term is enough to describe the G_p form factor:

$$G_p/f_s = g_p/f_s + g_p'/f_s \, q^2$$

and constants terms to describe the F_p and H_p form factors. The numerical results for all terms are given below:

$$
\begin{aligned}
f_s'/f_s &= 0.158 \pm 0.007_{\text{stat}} \pm 0.006_{\text{syst}} \\
f_s''/f_s &= -0.078 \pm 0.007_{\text{stat}} \pm 0.007_{\text{syst}} \\
f_e'/f_s &= 0.067 \pm 0.006_{\text{stat}} \pm 0.009_{\text{syst}} \\
f_p/f_s &= -0.049 \pm 0.003_{\text{stat}} \pm 0.004_{\text{syst}} \\
g_p/f_s &= 0.869 \pm 0.010_{\text{stat}} \pm 0.012_{\text{syst}} \\
g_p'/f_s &= 0.087 \pm 0.017_{\text{stat}} \pm 0.015_{\text{syst}} \\
h_p/f_s &= -0.402 \pm 0.014_{\text{stat}} \pm 0.008_{\text{syst}}
\end{aligned}
$$

The overall agreement between data and simulated distributions is excellent for each of the five kinematic variables as can be seen from Figure 2. The systematic errors quoted are conservatively taken from the 2003 data analysis [3] and are mainly due to background and acceptance uncertainties. They are being revisited for the final publication.

3.2 Determination of the scattering lengths

To extract scattering length values from the phase shift measurements of $(\delta = \delta_s - \delta_p)$, more theoretical ingredients are needed. The Roy equations [14], based on analyticity, unitary and crossing symmetries, allow to predict the $\pi\pi$ phase values close to threshold using experimental measurements above the matching point ($E = 0.8$ GeV) and two subtraction constants, a_0 and a_2, the
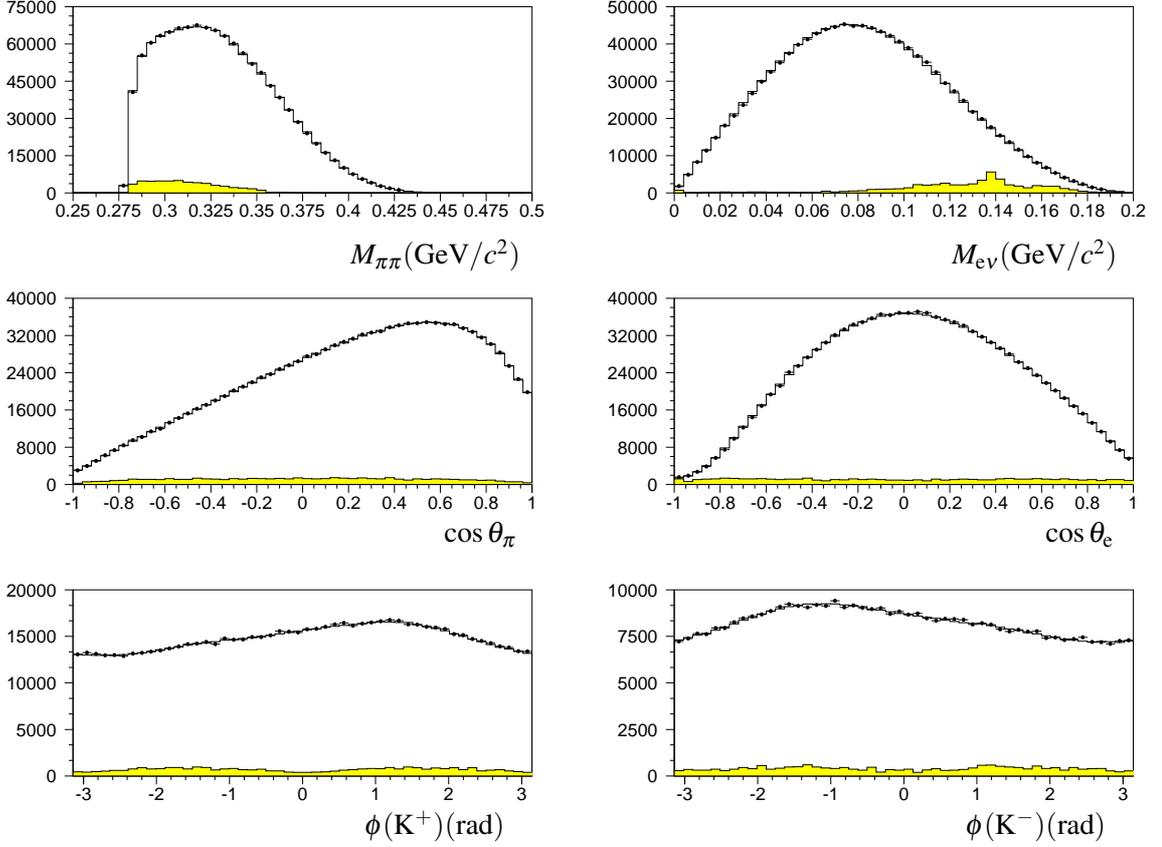
Figure 2: Distributions of the five Cabibbo-Maksymowicz variables The ϕ distributions are shown separately for K^+ and K^- to emphasize their opposite behavior. Data (after background subtraction) are shown as symbols with error bars, simulation using the fitted form factor values as histograms. The background contribution (WS events) is superimposed as shaded area, increased by a factor of 10 to be visible on the linear scale.

isospin 0 and 2 S-wave scattering lengths (in units of m_{π^+}). In a reverse way, from measurements of the phases and using the Roy equations, one can find the corresponding values of the subtraction constants. Numerical solutions of the Roy equations have been developed by several groups [15, 16] and can be used for that purpose. Recent theoretical work, triggered by NA48/2 preliminary results, has shown that isospin symmetry breaking may also alter the phases measured in the K_{e4} decays when all mass effects ($m_{\pi^+} \neq m_{\pi^0}, m_u \neq m_d$), neglected so far in the analyses, are considered [6]. Figure 3 left shows the effect of the above mass differences on the phase. The simultaneous determination of both scattering lengths a_0 and a_2 translates into a 68%CL contour in the (a_0, a_2) plane as shown in Figure 3 right. The wide Universal Band corresponds to the range of allowed solutions from the experimental inputs at high energy, while the narrow band corresponds to an additional constraint from Chiral Perturbation Theory (ChPT) [17]. The experimental phase measurements translate in a 2-parameter fit as:

$$a_0 = \quad 0.218 \quad \pm\, 0.013_{\text{stat}} \pm 0.007_{\text{syst}} \quad \pm\, 0.002_{\text{theo}} \,,$$
$$a_2 = -0.0457 \pm 0.0084_{\text{stat}} \pm 0.0041_{\text{syst}} \pm 0.0030_{\text{theo}} \,.$$

with a 97% correlation coefficient. Using the ChPT constraint ($a_2 + 0.0444 = 0.236(a_0 - 0.22) - 0.61(a_0 - 0.22)^2 - 9.9(a_0 - 0.22)^3 \pm 0.0008$), the value from the 1-parameter fit translates as:

$$a_0 = 0.220 \pm 0.005_{\text{stat}} \pm 0.002_{\text{syst}} \pm 0.006_{\text{theo}}$$

The theoretical error has been estimated by the authors of [6] and is dominated by the experimental precision of the inputs to the Roy equation and the neglected Higher Order loops when introducing the mass effects. This result can be compared to the most precise prediction of ChPT which uses additional inputs related to the Low Energy Constants (LEC) of the theory [17]:

$$a_0 = 0.220 \pm 0.005_{\text{theo}}$$
$$a_2 = -0.0444 \pm 0.0010_{\text{theo}}$$
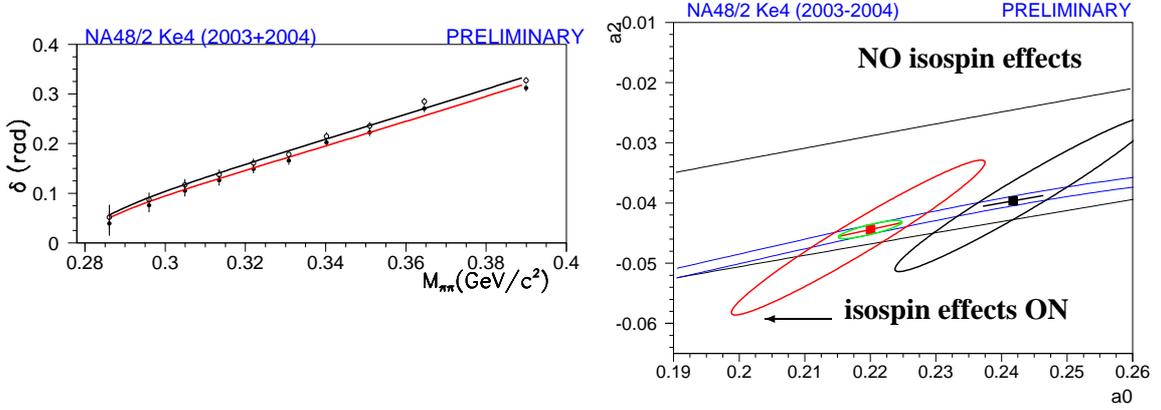
Figure 3: Left: Phase shift (δ) measurements without mass effects (top black line) and with mass effects included (bottom red line). In each case the line corresponds to the 2-parameter fit. Right: Fits of the NA48/2 K_{e4} data in the (a_0, a_2) plane without (black) and with (red) isospin mass effects. The symbols are the result of the one-parameter fit imposing the ChPT constraint. The small (green) ellipse corresponds to the most accurate prediction from ChPT.

4. The $K_{3\pi}$ decay analysis

Events with at least one charged track and at least four energy clusters in LKr consistent with a photon are selected. The pairing of two photons under the assumption of a π^0 decay defines the longitudinal position of the decay vertex $Z_{ik} = \sqrt{E_i E_k D_{ik}^2}/m_0$ where E_i, E_k are the energies of the i-th and k-th photon, respectively, D_{ik} the distance between the impact points on LKr, and m_0 is the π^0 mass. The $K^\pm$ decay vertex Z position is defined as the mean of the two pairings. The additional charged track is assumed to be a $\pi^\pm$ and is used to compute the Kaon mass. The best two photons pairings which minimize the distance between the two π^0 decay vertices and the difference between the reconstructed Kaon mass and the nominal $K^\pm$ mass are chosen. Figure 4 left shows the invariant mass distribution of the reconstructed $K^\pm$ mass.

4.1 Rescattering effects

The original aim of the analysis of $K_{3\pi}$ decays close to $2m_{\pi^+}$ threshold was the search for the decay $K^\pm \to (\pi^+\pi^-)_{atom}\pi^\pm$ with the subsequent decay of the pionium atom $(\pi^+\pi^-)_{atom}$ into $\pi^0\pi^0$. The observed cusp in the M_{00}^2 distribution (Figure 4 right) was interpreted as strong rescattering from the $K^\pm \to \pi^+\pi^-\pi^\pm$ decay and has been evaluated at one- and two-loop orders [7, 8, 18].
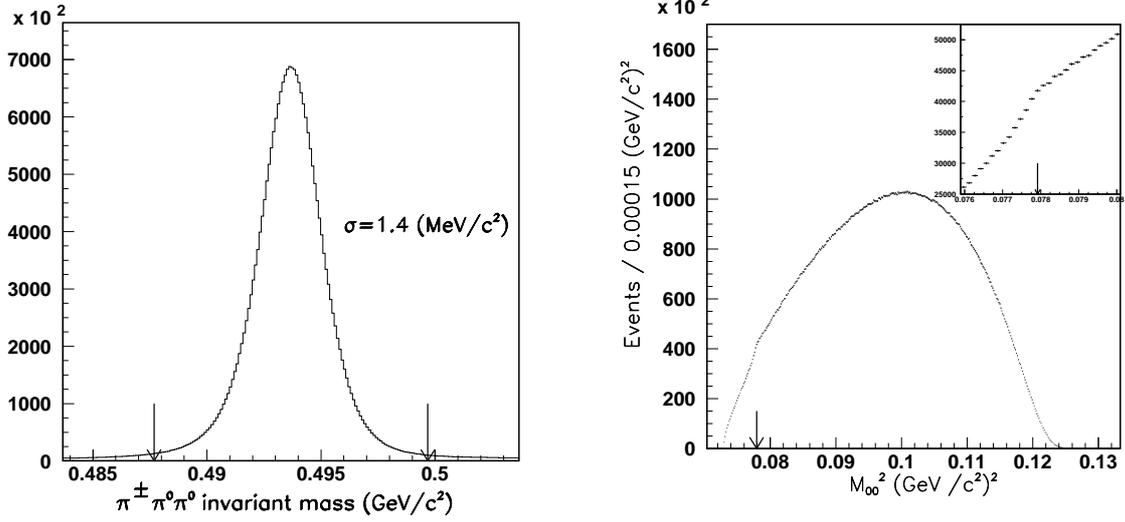
Figure 4: Left: Invariant mass distribution of reconstructed $\pi^\pm\pi^0\pi^0$ candidate events. The arrows indicate the selected mass interval. Right: invariant $\pi^0\pi^0$ mass squared and zoom in the cusp region.

At one loop, the $\mathcal{M}_0$ unperturbed amplitude is to be supplemented by the rescattering amplitude $\mathcal{M}_1$, imaginary above threshold. Below threshold $\mathcal{M}_1$ becomes real and negative, inducing a destructive interference term which explains the leading effect. Subleading effects from two-loop graphs affect also the distribution above threshold. The formulation used here is different from the PDG one and reads:
$\mathcal{M}_0 = A_0(1 + \frac{1}{2}g_0u + \frac{1}{2}h'_0u^2 + \frac{1}{2}k'_0v^2)$, $\mathcal{M}_1 = \frac{-2}{3}(a_0 - a_2)m_{\pi^+}\mathcal{M}_+\sqrt{1 - (M_{00}/2m_{\pi^+})^2}$,
and $\mathcal{M}_+ = A_+(1 + \frac{1}{2}g_+u + \frac{1}{2}h'_+u^2 + \frac{1}{2}k'_+v^2)$ for the $K^\pm \to \pi^+\pi^-\pi^\pm$ amplitude.
The k'_0 value is fixed from a 2-dimensional fit of the $K^\pm \to \pi^0\pi^0\pi^\pm$ Dalitz plot, far from the cusp region. In the full statistics analysis, the fit range has been extended to larger values by 50 bins (bin width is $0.00015(\text{GeV}/c^2)^2$) which represents a fair compromise between statistical error and systematic error contributions. As in the analysis of a partial data sample [4], seven bins around the $2m_{\pi^+}$ threshold are excluded to avoid the effects of the strong Coulomb attraction between the two charged pions, not included in the models. Two theoretical approaches have been developed using different formalisms and ingredients [7, 8]. In both approaches, the M_{00}^2 distribution is fitted, using the detector response matrix obtained from a large Monte-Carlo simulation, to extract the scattering lengths $a_0 - a_2$, a_2 and the Dalitz plot slopes g_0 and h'_0.

4.2 Scattering lengths extraction

In the Cabibbo-Isidori approach (labeled CI [7]), both one- and two-loop effects are included. Radiative corrections are not yet included and a theoretical uncertainty of 5% is quoted to acount

7

for missing ingredients. The $\mathcal{M}_+$ amplitude of the $K^\pm \to \pi^+\pi^-\pi^\pm$ is obtained from a fit to the Dalitz plot measured by NA48/2 [10]. The scattering lengths are extracted together with the Dalitz plot parameters of the $K^\pm \to \pi^0\pi^0\pi^\pm$ decays.

In the Bern-Bonn approach (labeled BB [8]), an effective field theory is used, based on a non-relativistic Lagrangian. The two-loop formulation is different from the CI expressions therefore introducing different correlations between the scattering lengths and the Dalitz plot parameters. Electromagnetic effects have been recently included in the amplitudes, and the study of their impact is in progress. The $\mathcal{M}_+$ amplitude is obtained here from a simultaneous fit of both $K^\pm \to \pi^+\pi^-\pi^\pm$ and $K^\pm \to \pi^0\pi^0\pi^\pm$ Dalitz plots within the same code. The fitted slopes are thus different from those used in the CI approach.

The numerical results for all terms are given below from a fit using the ChPT constraint between a_0 and a_2 and without electromagnetic corrections:

	CI model	*BB model*	*errors*
$k'_0 =$	0.0095	0.0095	$\pm 0.0002_{\text{stat}} \pm 0.0005_{\text{syst}}$
$g_0 =$	0.652	0.621	$\pm 0.001_{\text{stat}} \pm 0.003_{\text{syst}}$
$h'_0 =$	-0.039	-0.049	$\pm 0.001_{\text{stat}} \pm 0.003_{\text{syst}}$
$a_0 - a_2 =$	0.268	0.266	$\pm 0.003_{\text{stat}} \pm 0.002_{\text{syst}} \pm 0.001_{\text{ext}}$

The external error is mainly due to the ratio $R = A_+/A_0 = 1.975 \pm 0.015$ which does not include yet the Coulomb corrections and is expected to change slightly in the final analysis. If the a_2 parameter is left free in the fit, the values become:

	CI model	*BB model*
$a_0 - a_2 =$	$0.266 \pm 0.005_{\text{stat}} \pm 0.002_{\text{syst}} \pm 0.001_{\text{ext}}$	$0.273 \pm 0.005_{\text{stat}} \pm 0.002_{\text{syst}} \pm 0.001_{\text{ext}}$
$a_2 =$	$-0.039 \pm 0.009_{\text{stat}} \pm 0.006_{\text{syst}} \pm 0.002_{\text{ext}}$	$-0.065 \pm 0.015_{\text{stat}} \pm 0.010_{\text{syst}} \pm 0.002_{\text{ext}}$

The two measurements are shown in Figure 5 in both $(a_0 - a_2, a_2)$ and (a_0, a_2) planes for the free a_2 fit (68% CL contour) and the constrained fit. Both contours have an overlap in the region of the ChPT constraint band.

5. Results and comparisons

From the analysis of more than one million K_{e4} decays and using dedicated theoretical calculations of rescattering effects on the measured $\pi\pi$ phases, an improved determination of the S-wave scattering lengths a_0 and a_2 has been achieved. Consistent results are obtained both in the 2-parameter fit and in the constrained 1-parameter fit, favouring the most precise predictions of the ChPT: $a_0 = 0.220 \pm 0.005_{\text{theo}}$, $a_2 = -0.0444 \pm 0.0010_{\text{theo}}$. The experimental precision is now at the same level as the theoretical precision. Because K_{e4} analyses have been conducted in independent $M_{\pi\pi}$ bins and without relying on any specific model, the corrections due to neglected mass effects can be applied retro-actively to previous results. Even if the experimental uncertainty is larger than the mass effects, the central value moves according to a coherent shift. Using the ChPT constraint, the value obtained for each of the K_{e4} experiments is shown on Figure 6. If the Geneva-Saclay result is fully compatible within a large uncertainty, the more precise measurement
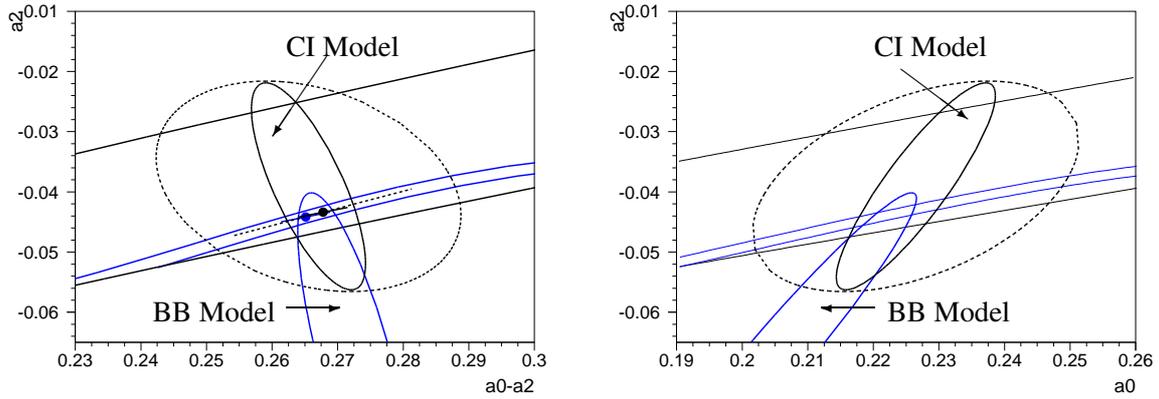
Figure 5: Left: $K_{3\pi}$ NA48/2 measurements in the $(a_0, a_0 - a_2)$ plane for the two models. Right: same result transformed to the (a_0, a_2) plane. In both planes, the narrow band corresponds to the ChPT constraint and the points inside the band to the use of this additional input. The dotted contour corresponds to an additional 5% theoretical uncertainty to the CI Model.

of the E865 experiment is marginally consistent, in particular the highest energy point is responsible for most of the disagreement. The analysis of more than ~ 60 millions $K_{3\pi}$ decays has triggered several theoretical developments to model rescattering effects. Work is still going on to implement all ingredients, in particular the electromagnetic effects. When imposing the ChPT constraint, both models give consistent results in agreement with the K_{e4} results and the ChPT prediction. The result from the DIRAC experiment, sensitive to $|a_0 - a_2|$ through the pionium life time measurement and based on part of the accumulated statistics, is also shown in Figure 6.
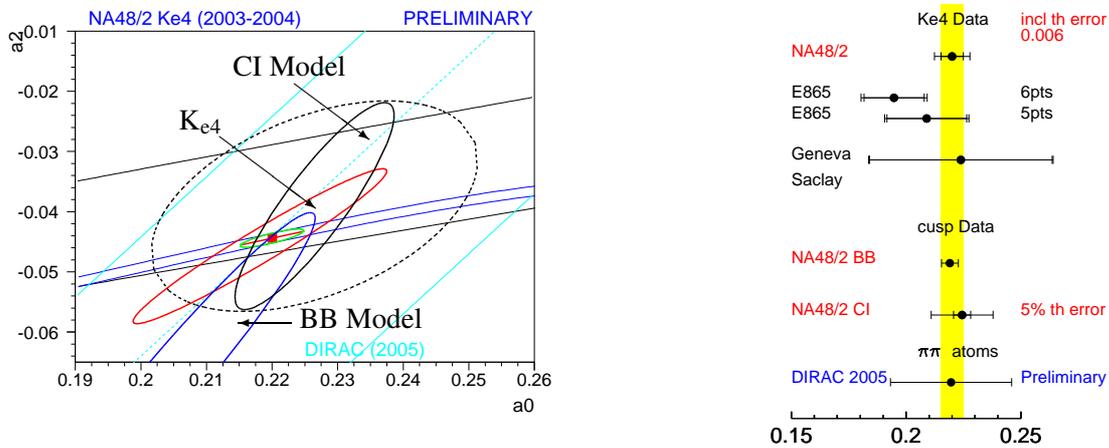
Figure 6: Left: results from K_{e4} and $K_{3\pi}$ NA48/2 measurements in the (a_0, a_2) plane. The dotted ellipse corresponds to an additional 5% error from missing theoretical ingredients. Right: All available measurements of a_0 using the ChPT constraint.

6. Conclusion

The NA48/2 experiment has analyzed more than one million K_{e4} decays and ~ 60 millions

$K_{3\pi}$ decays to extract the isospin 0 and 2 S-wave $\pi\pi$ scattering lengths . With the help of dedicated theoretical calculations, developed in close collaboration between experiment and theory, precise results have been obtained:

$$K_{e4} : a_0 = 0.220 \pm 0.005_{\text{stat}} \pm 0.002_{\text{syst}} \pm 0.006_{\text{theo}},$$
$$K_{3\pi} : a_0 - a_2 = (0.266 - 0.268) \pm 0.003_{\text{stat}} \pm 0.002_{\text{syst}} \pm 0.001_{\text{ext}} \pm 0.013_{\text{theo}},$$

confirming the predictions of Chiral Perturbation Theory:

$$a_0 = 0.220 \pm 0.005_{\text{theo}} , a_2 = -0.0444 \pm 0.0010_{\text{theo}}.$$

References

[1] L. Rosselet et al., Phys. Rev. **D15** (1977) 574.

[2] S. Pislak et al., Phys. Rev. Lett.**87** (2001) 221801, Phys. Rev. **D67** (2003) 072004.

[3] J. Batley et al., Eur. Phys. J. **C54** (2008) 411.

[4] J. Batley et al., Phys. Lett. **B633** (2006) 173.

[5] V. Fanti et al., *Nucl. Inst. Methods* **A574** (2007) 433.

[6] G. Colangelo, J. Gasser and A. Rusetsky, arXiv:0811.0775, accepted by EPJC.

[7] N. Cabibbo, Phys. Rev. Lett.**93** (2004) (12181), N. Cabibbo and G. Isidori, JHEP 0503(2005) 021.

[8] G. Colangelo, J. Gasser, B. Kubis and A. Rusetsky, Phys. Lett. **B638** (2006) 187,
M. Bissegger, A. Fuhrer, J. Gasser, B. Kubis and A. Rusetsky, Phys. Lett. **B659** (2008) 576,
M. Bissegger, A. Fuhrer, J. Gasser, B. Kubis and A. Rusetsky, Nucl. Phys. **B806** (2009)(178) .

[9] B. Adeva et al., Phys. Lett. **B619** (2005) 50.

[10] J. Batley et al., Phys. Lett. **B649** (2007) 349.

[11] N. Cabibbo and A. Maksymowicz, Phys. Rev. **137** (1965) B438; Phys. Rev. **168** (1968) 1926.

[12] A. Pais and S. Treiman, Phys. Rev. **168** (1968) 1858.

[13] E. Barberio and Z. Was, PHOTOS, Comp. Phys. Comm. **79** (1994) 291,
G. Nanava and Z. Was, Eur. Phys. J. **C51** (2007) 569,
P. Golonka and Z. Was, Eur. Phys. J. **C45** (2006) 97.

[14] S. Roy, Phys. Lett. **B36** (1971) 353.

[15] B. Ananthanarayan, G. Colangelo, J. Gasser, H. Leutwyler, Phys. Rept. **353** (2001) 207.

[16] S. Descotes, N. Fuchs, L. Girlanda, J. Stern, Eur. Phys. J. **C24** (2002) 469.

[17] G. Colangelo, J. Gasser, H. Leutwyler, Nucl. Phys. **B603** (2001) 125,
G. Colangelo, J. Gasser, H. Leutwyler, Phys. Rev. Lett.**86** (2001) 5008

[18] U.G. Meissner, G. Muller and S. Steininger, Phys. Lett. **B406** (1997) 154, Erratum
ibid. **407** (1997) 454.